

# Synthesis of smart core–shell polymer in supercritical carbon dioxide

Liqin Cao, Liuping Chen <sup>\*</sup>, Xiaojuan Chen, Lihua Zuo, Zhiwei Li

*School of Chemistry and Chemical Engineering, Sun Yat-Sen University, Guangzhou, Guangdong 510275, People's Republic of China*

Received 3 December 2005; received in revised form 28 February 2006; accepted 23 April 2006

Available online 18 May 2006

## Abstract

Herein we report a new and simple method that has been developed to prepare smart polymeric microgels consisting of temperature-sensitive cores with pH-sensitive shells. The microgels were obtained directly from one step seed polymerization of *N*-isopropylacrylamide and *N,N*-methylenebisacrylamide from water-soluble biopolymers containing carboxymethyl groups in supercritical carbon dioxide. The effect of initial concentration of initiator, crosslinker, and carboxymethyl starch (CMS) dose as well as reaction pressures on the yield and morphology of the resulting polymer were investigated. CMS and crosslinker worked effectively as surfactant to some extent. PNIPAM/CMS particles with diameters in 100 nm and narrow particle size distribution were produced in supercritical carbon dioxide, in high yield and in short reaction times. © 2006 Elsevier Ltd. All rights reserved.

*Keywords:* Carboxymethyl starch (CMS); *N*-Isopropylacrylamide; Seed polymerization

## 1. Introduction

Supercritical fluids (SCF) can exhibit the best features of two worlds: they can have gaslike diffusivities and liquidlike densities. In the vicinity of the fluid's critical point, its density is highly sensitive to modest changes in pressure or temperature. Higher SCF diffusivities have important implications in polymerization kinetics and in polymer processing (i.e. diminishing the 'cage effect' associated to the initiator decomposition in free radical polymerization processes). The resulting polymer can be isolated from the reaction medium by simple depressurization, resulting in a dry, solvent-free product. This technique eliminates drying procedures required in polymer manufacturing, offering a cost-effective and very attractive technology. The thermodynamic and transport properties of SCFs can be easily tuned by adjusting the pressure or temperature. It can dissolve small organic molecules, and can swell most polymers.

scCO<sub>2</sub> has near-zero surface tension and large diffusion coefficient. Therefore, it can be used to impregnate polymer matrix with different organic molecules. This principle has been used to modify different polymers [1–12]. However, so far more attention is only put in the graft products of synthetic polymers. To the best of our knowledge, in the literatures, no

previous attempt appears to have been made to study core–shell polymers based from biopolymers in scCO<sub>2</sub>. Besides, limited research efforts have been reported on the polymerization of water-soluble vinylic monomers containing acylamide in carbon dioxide, including inverse emulsion polymerization of acrylamide [13,14], emulsion polymerization of *N*-ethylacrylamide [15], dispersion copolymerization of *N,N*-dimethylacrylamide [16].

As for synthesis of core–shell polymers in scCO<sub>2</sub>, there are numerous possible particle morphologies, or distributions of the two polymer phases in the final particles. Other morphologies include inverted, sandwich, raspberry, and half-moon. A balance between thermodynamic and kinetic factors determines the morphology of the resulting particles [17].

Environmental stimuli-responsive polymeric hydrogels attract increasing attention in numerous fields for their potential applications [18–26]. The representatives of the stimuli-responsive polymers are P(*N*-isopropylacrylamide) (PNIPAM) and its copolymers. Temperature- and pH-sensitive hydrogels are the most investigated, because of the easy control and wide-ranging applicability of these signals such as in biotechnology, chemical processing, and medical fields [27]. Generally, the free radical emulsion polymerization technique is limited to the use of a pH-responsive vinylic monomer. The amount of pH-sensitive comonomer greatly affects the volume phase transition temperature (VPTT) of the microgels. To address this limitation, we describe a one-step seed polymerization using scCO<sub>2</sub> medium to produce novel nano-sized

<sup>\*</sup> Corresponding author. Tel.: +86 20 8411 5559; fax: +86 20 8411 2245.  
E-mail address: [cesclp@zsu.edu.cn](mailto:cesclp@zsu.edu.cn) (L. Chen).

core-shell stimuli-responsive polymers directly from a pH-sensitive biopolymer, carboxymethyl starch. Hence their responsiveness to pH and temperature can be manipulated individually. Because of the presence of stabilizers that cannot be easily removed from the polymer becomes a concern for some applications. Precipitation polymerization is an alternative approach, which produces stabilizer-free polymers [28].

Chemically modified starches with improved properties are gaining increasing importance in industry not only because they are low in cost, but also mainly because the polysaccharide portion of the product is biodegradable. Their applications relate to agriculture, industry, medical treatment and sanitation, and so on, which make them important polymeric materials in the fields of dehumidification, dehydration, water preservation and water absorption.

Since  $\text{scCO}_2$  behaves a series of advantages as green medium mentioned above, it can be used to impregnate polymer matrix with different organic molecules. Polymeric particle coating finds wide applications in various important industries: pharmaceutical, food, fertilizer, cosmetics, electronic, and biomedical, just to name a few. It is often a crucial industrial process in particle handling to enhance compatibility, flowability, wettability, and dispersibility, or to serve as a barrier for controlled release or masking. Conventional polymeric particle coating usually involves solution chemistry and the use of a large amount of organic solvents may raise serious air and water pollution concerns. Therefore, effective and clean coating methods are of strong interest. This idea gives further understanding to the one-step seed polymerisation of smart hydrogels using CMS in  $\text{scCO}_2$ .

The objectives of the study are (i) to show that  $\text{scCO}_2$  can dissolve CMS to some extent in the presence of monomers and (ii) to find a new route towards materials that can be applied in biomedicine. In this study, the initiator, crosslinker, CMS dose, reaction pressure effect on the resulting polymers were explored.

## 2. Experimental

### 2.1. Materials

The monomer *N*-isopropylacrylamide (NIPAM) was purchased from Acros (99%) and was used as received. 2,2'-Azobis (isobutyronitrile) (AIBN) was supplied by Shanghai Chemical Agent fourth Factory and was recrystallized twice from methanol. Commercially maize starch was dried at 60 °C for 2 h before being used. *N,N*-Methylenebisacrylamide (MBAM) was analytical reagent grade and supplied by Tianjin Chemical Reagent Company. Chloroacetic acid was analytically pure and purchased from the Shantou Reagent Factory, China. Sodium hydroxide, methanol, ethanol and hydrochloric acid were analytical reagent grade and supplied by the Guangzhou Chemical Reagent Factory; carbon dioxide gas was purchased from Guangzhou Gas Factory with >99.95% purity. High-pressure reactions were carried out in a 300 mL stainless steel reactor equipped with sapphire windows used for observation of the phase behavior during the reaction process.

The pressure in the reactor was measured using a pressure gauge in the range of 0–400 bar. The temperature of the reactor was measured with a platinum resistance thermometer (model WMZK-01, produced by Shanghai medical instruments Factory). A magnetic stirrer was used for mixing.

### 2.2. Preparation of CMS

The procedures for preparing water-soluble CMS have been described in Ref. [29]; sodium content, and hence the degree of substitution (DS) of carboxymethyl groups in the CMS, was measured with cinefaction method. And the DS of CMS can be calculated based on the following equation

$$\text{DS} = \frac{162W_{\text{Na}}}{23 - 81W_{\text{Na}}}$$

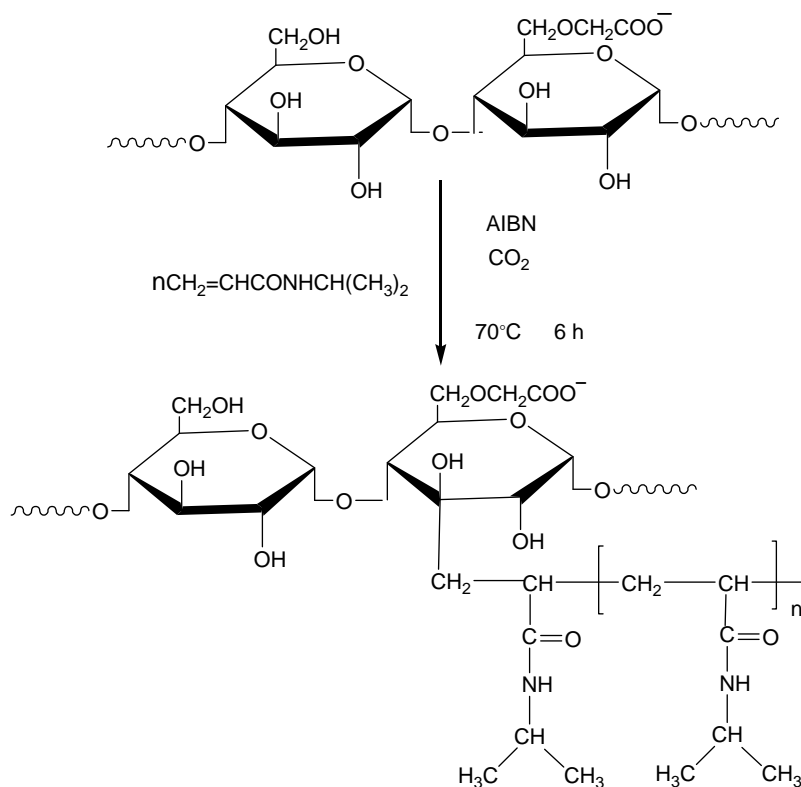
Where 162, 23 and 81 are the relative molecular masses of dehydration glucose, sodium atom and substituent group, respectively.

### 2.3. Graft copolymerization

The synthetic procedure used to conduct the polymerization is shown in Scheme 1. In a typical experiment, the known amounts of CMS (DS=0.21), solid monomer, the free-radical initiator AIBN and crosslinker MBAM were loaded to the reaction vessel. Next, the reactor immersed in an ice bath was first purged with a flow of  $\text{CO}_2$  to remove any entrapped air from the vessel and then filled with liquid  $\text{CO}_2$  to desired amount (222 g), after charging, the system was isolated and the reactor was gradually heated to 70 °C, and the pressure was increased to approximately 260 bar, with a stick-shaped stir bar agitated the mixture. On average, it took approximately 120 min to heat from room temperature to 70 °C, The reaction conditions were maintained at 70 °C, 260 bar during the reaction time. At the end of the reaction, the system was then cooled to room temperature, and  $\text{CO}_2$  was slowly vented. The physical form and the overall appearance of the polymer were noted. The polymer was then transferred to a high-vacuum chamber to remove any unreacted monomer residues. The yield of the polymer product was determined gravimetrically.

### 2.4. Measurement and characterization

The VPTTs of the microgels were determined by measuring the light transmittance (at 500 nm) of a microgel dispersion between 24 and 42 °C using CARY 100 UV-vis spectrophotometer (Varian, Inc., USA), equipped with a circulating water bath. scanning electron microscopy (SEM) images were obtained using a JSM-6330 FE SEM (JEOL Ltd, Japan). The hydrodynamic radius ( $R_h$ ) of the microgels was measured by dynamic light scattering (DLS) (BI-200SM goniometer and BI-900AT digital correlator, Brookhaven Instruments, Holtsville, NY) at 25 °C; The core-shell nanostructures of the microgels were observed using a transmission electron microscope (JEM-2010HR, JEOL LTD, Japan) at an accelerating voltage of



Scheme 1. Graft copolymerization of CMS with NIPAM.

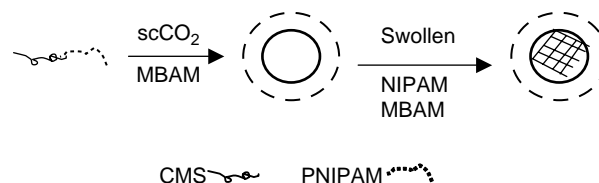
200 kV after treating the particles with 2% phosphotungstic acid (PTA). FTIR spectra of PNIPAM, CMS and copolymer samples were taken in KBr pellets using a Bruker/VECTOR 22 FTIR spectrophotometer (Bruker Optics, Inc., Germany). The pH sensitivity was measured by swelling ratios in different pH buffers. Copolymer particles were immersed in the buffers of various pH values from 4.6 to 9 for 2 weeks.

### 3. Results and discussions

#### 3.1. Synthesis of core-shell microgels

In precipitation polymerization, the monomer(s) and initiator are soluble in the continuous phase and the polymer precipitates as it is formed, often as an undefined, agglomerated powder. Dispersion polymerization is also characterized by initially homogeneous conditions. However, the resulting insoluble polymer is stabilized as a colloid by use of appropriate surfactants to give spherical polymer particles in the size range 100 nm to 10  $\mu\text{m}$ . In stabilized reactions, residual surfactant on particle surfaces may sometimes impair the performance properties of the resulting polymers. Therefore, in this work, the smart particles of PNIPAM/CMS were produced in the absence of surfactant. In heterogeneous processes, two polymerization loci are expected to contribute to the polymer production: the  $\text{CO}_2$ -rich continuous phase and the polymer-rich dispersed phase. The mass transport of reactants between phases is the key factor in determining the relative importance of each polymerization locus.

The core-shell particles were prepared by the graft copolymerization of NIPAM from CMS at  $70^\circ\text{C}$  in  $\text{scCO}_2$ . (Scheme 2) Primary radicals are formed from thermally promoted fragmentation of the initiator AIBN. The radicals in the medium that cleaves a hydrogen from the starch main chain and creates active sites on the starch macromolecules, which then initiated both the graft copolymerization and the homopolymerization of NIPAM concurrently in the presence of a crosslinker, *N,N*-methylenebisacrylamide. At the beginning, the only active locus is the continuous phase, where the first polymer chains are produced. Thus the PNIPAM became ' $\text{CO}_2$ -phobic' and phase-separated during the polymerization. The negative PNIPAM-*g*-CMS generated in situ thus acted like anionic polymeric surfactants, self-assembling to form micelle-like microdomains, because of the very limited stability of the microdomains, they rapidly aggregate to form primary polymer particles. From this point on, the polymerization proceeds in two phases, namely, the polymer-rich phase and the  $\text{CO}_2$ -rich phase. However, as soon as particles are formed, monomer, initiator and active species are partitioned between the continuous and polymer phases and both loci are effective.

Scheme 2. Presentation of the formation of core-shell NIPAM/CMS in  $\text{scCO}_2$ .

Under stable conditions, the particles very rapidly become the dominant locus. The polymerization continues only in the polymer-rich phase, which is swollen with monomers (NIPAM and crosslinker) and CO<sub>2</sub>. Then the core portion of the particles was formed. During this stage, diffusion-controlled phenomena become very important. This mechanism is supported by most researchers.

### 3.2. FT-IR spectroscopic studies

The IR spectra of pure starch and PNIPAM/CMS as shown in Fig. 1 indicated that both have a broad absorption band characteristic of glucosidic ring of starch between 3700 and 3200, 1640, 1160 cm<sup>-1</sup>. Moreover, there is an increment in the intensity of these bands in the case of a PNIPAM/CMS sample. The absorption maxima of amide I groups (i.e. amide I: C=O stretching and amide II: N–H bending) of PNIPAM/CMS are located in 1654 cm<sup>-1</sup>. The stretching vibration peak due to CO groups in CMS repeats units are located between 1800 and 1600 cm<sup>-1</sup> broad absorption band. The spectrum indicates clearly that the grafting process has taken place.

### 3.3. Phase behavior of the reaction mixture

The phase of the CO<sub>2</sub>/monomer/biopolymer system was investigated by coupling visual observation of the mixture to the recording of the pressure trend inside the fixed volume view autoclave as a function of the temperature during the slow heating of the reaction system. At room temperature, all the investigated systems were composed of two fluid phases, which merged into a single phase during the heating cycle.

This simple static synthetic method was repeated for all initial feed compositions of the reaction mixture adopted in this work, all of which were initially composed of a single phase under the operating conditions adopted to perform the polymerization. During graft copolymerization of CMS with PNIPAM at very low monomer concentrations (0.8 g NIPAM, 236 g CO<sub>2</sub>) the polymerization mixture was initially all clear and homogeneous (25 °C, 85 bar). The solution was gradually heated (to 70 °C, 330 bar), and after 45–60 min an orange/red color was observed, due to scattering of transmitted light by the

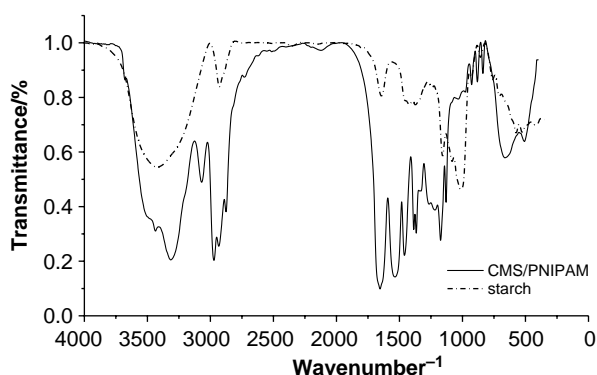


Fig. 1. FTIR spectra of starch, copolymers PNIPAM/CMS synthesized in present study.

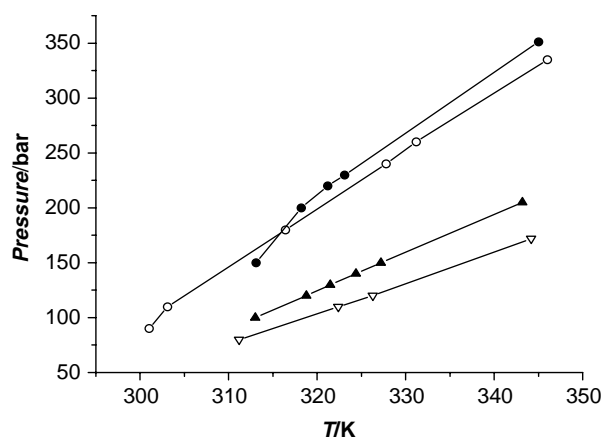


Fig. 2. Record of pressure inside the view cell as a function of temperature. System composition: 0.8 g NIPAM, 0.25 g CMS. Density: (∇) curve 1, 0.61 g cm<sup>-3</sup> (▲) curve 2, 0.70 g cm<sup>-3</sup> (○) curve 3, 0.80 g cm<sup>-3</sup> (●) curve 4, 0.83 g cm<sup>-3</sup>.

growing polymer particles (i.e. the Tyndall effect). The clear solution developed a white opaque after 3 h, and precipitate formation was observed after 4 h. Fig. 2 shows the variation of pressure as a function of temperature is good linear over the studied temperature. It was observed that, at fixed molar fractions of the components, with increase the average density (defined as the sum of the masses of CO<sub>2</sub>, NIPAM, divided by the free volume of the view autoclave) of the reaction system, the polymer particles mainly distribute change from windows and walls to bottom of the autoclave gradually.

### 3.4. The effect of the initiator AIBN concentration

We have investigated the concentration of initiator over the range 2.6–6.25 wt% with respect to monomer at constant feed compositions, and the results obtained are summarized in Table 1. When the polymerization was conducted with lower initiator concentration (2.6 wt%), there is no homogeneous white powder, but little sticky highly coagulated product was obtained (entry 3). However, when the initiator concentration is 6.25 wt%, the conversion is up to 75%. This increasing trend of graft yield is attributed to the creation of a greater number of reaction sites arising from an increase in the concentration of AIBN in the reaction system, where rather high initiator concentrations seemed necessary to achieve good monomer conversions.

Table 1  
Effect of CMS/NIPAM ratio on graft copolymerization in scCO<sub>2</sub>

Entry	CMS/NIPAM/ (w/w)	Conversion (%)
1	1.3/10	63.59
2	3.1/10	74.67
3 <sup>a</sup>	3.1/10	20.5
4	4.4/10	91.43

Reaction condition: 0.8 g NIPAM, 0.025 g MBAM, 0.05 g AIBN, 260 bar, 70 °C, 6 h.

<sup>a</sup> 2.6% w/w AIBN based on monomer.



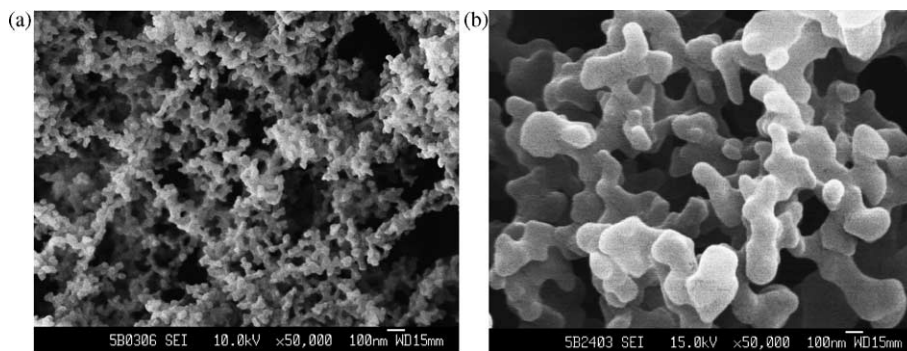


Fig. 3. The effect of NIPAM/CMS ratio. (a) 0.15 g CMS; (b) 0 g CMS.

### 3.5. The effect of the CMS/NIPAAAM weight ratio

Two general trends were obtained. First, the core-shell particles were similar in size to that of formed by dispersion polymerization in  $scCO_2$  in the presence of stabilizers, although there was considerably more evidence of particle agglomeration in our samples. Free flowing powders were obtained in all case. At CMS/NIPAM weight ratio 1.3/10 relatively uniform partially aggregated microspheres were obtained with diameters mostly in 50 nm (Fig. 3(a)). In the absence of CMS, larger, agglomerated structures were observed (entry 9, Fig. 3(b)). The second notable trend was a strong dependence of conversion on CMS amount. Table 1 shows the effect of the CMS/NIPAAAM weight ratio on the conversion of copolymerization after 3 h of reaction. The results showed that the increase in the CMS/NIPAAAM weight ratio increased the conversion of copolymerization. This may be attributed to the fact that, with the increase in CMS amount, the number of reaction sites for grafting increases, thus resulting in an increase in conversions. Besides, The CMS behaved as a surfactant, preventing polymer particles from coagulation, thereby decreasing the particle diameter and increasing the particle number. This is consistent with studies by Lee [30,31] Fig. 4.

The dry polymer particles (entry 2) were observed by TEM, and the water-swollen particle diameters were measured by dynamic light scattering at 25 °C; The diameters of the water-swollen polymer particles measured by dynamic light scattering were much larger than those observed by TEM, as expected. Dynamic light scattering measurement indicated that

average volume diameters of PNIPAM/CMS particles at pH 7 produced after the polymerization was 420 nm (Fig. 5). The polydispersity index was 0.10, indicating a narrow size distribution of the microgels. With careful staining of the particles, the nanostructures of the microgels were revealed with TEM micrographs. Fig. 6 shows that the microgels are approximately spherical and have well-defined core-shell morphologies where PNIPAM cores are coated with CMS shells.

### 3.6. The effect of crosslinker dose

In the absence of crosslinker, the precipitation graft copolymerization of NIPAM onto CMS in  $scCO_2$  resulted in poor yield (Table 2, entry 5). Fig. 4 shows the effect of the amount of the crosslinker on the morphology of the polymer particles. Because the crosslinking structure reduced the solubility of PNIPAAAM chains in  $scCO_2$ , the polymers with a higher degree of crosslinking precipitated out of the  $CO_2$  fluid phase faster. Therefore, the increase in the concentration of the crosslinking agent increased the number of nuclei generated in the reaction system and reduced the particle diameter, as shown in Fig. 4. In addition, it was assumed that the particle formation and growth mechanisms were similar to those of dispersion polymerization, except that the particles were stabilized against coagulation by their rigid, crosslinked surfaces rather than by added stabilizers [32]. We also think that the formation of microspheres in our samples attributes to the rigidity of the polymers. Since the homopolymerization of NIPAM without crosslinker was also studied, little yellow free flow solid

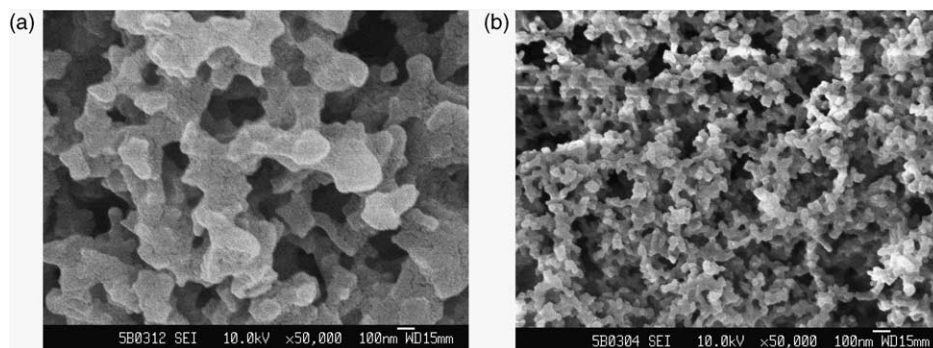


Fig. 4. The effect of crosslinker dose (a) 0.008 g MBAM (b) 0.025 g MBAM.

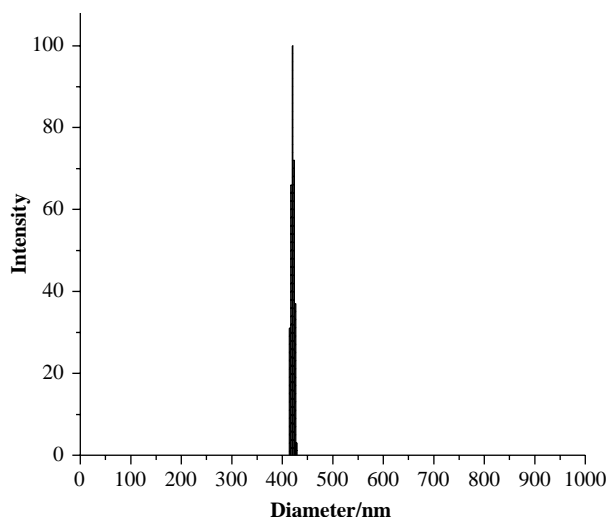


Fig. 5. Hydrodynamic diameter distribution of PNIPAM/CMS aqueous solution (0.2 mg/mL) at 25 °C analyzed with the CONTIN program ( $\theta=90^\circ$ ). Reaction conditions: 0.025 g MBAM; 0.25 g CMS; 0.8 g NIPAM; 0.05 g AIBN; 70 °C; 6 h.

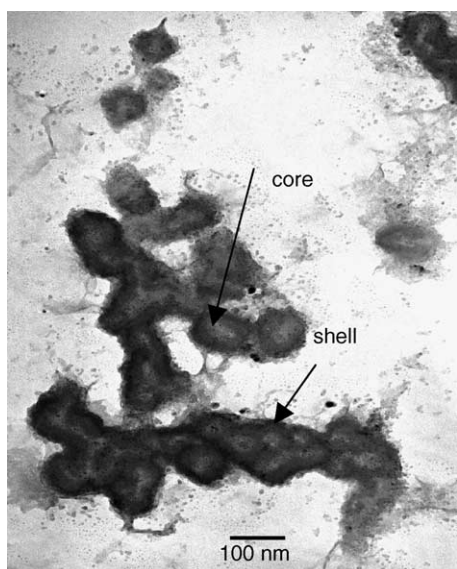


Fig. 6. TEM images of PNIPAM/CMS particles from the reactions at the  $\text{CO}_2$  pressure of 260 bar. Reaction conditions: 0.8 g NIPAM; 0.25 g CMS; 0.05 g AIBN; 70 °C; 6 h. 2% phosphotungstic acid (PTA) negatively stained.

Table 2  
Effect of crosslinker ratio on graft copolymerization in  $\text{scCO}_2$

Entry	Crosslinker (g)	Conversion (%)
5	0	41.67
6	0.008	65.79
7	0.025	74.67
8	0.04	85.61
9 <sup>a</sup>	0.04	73.37

Reaction condition: 0.8 g NIPAM, 0.25 g CMS, 0.05 g AIBN, 260 bar, 70 °C, 6 h.

<sup>a</sup> 0 g CMS.

particles were obtained. The morphology is very different from above samples. The fact that the lightly crosslinked polymers did not form microspheres (entry 6) is consistent with this idea. The particles formed from higher crosslinker agent samples (Fig. 4(b)) were significantly less agglomerated than those formed from lower crosslinker agent samples (Fig. 4(a)), perhaps because the highly crosslinked particles were more rigid, and therefore less prone to aggregation. Such similar phenomena are also found by other works [33].

### 3.7. The effect of the $\text{CO}_2$ pressure

An opportunity unique to supercritical fluids as a reaction medium is the ability to adjust its solvent quality through its easily tunable density and dielectric constant by simply changing either pressure or temperature. Moreover, for free-radical reactions,  $\text{CO}_2$  offers no chain transfer to solvent and high free-radical initiation efficiency with acceptable initiator decomposition kinetics [34]. The precipitation graft copolymerization of PNIPAM/CMS in  $\text{scCO}_2$  was conducted at three different pressures; the results are collected in Table 3.

All reactions were performed with the same amount of monomer, initiator (6.25 wt% based on the monomer weight), at 70 °C for 6 h. During the reactions, the corresponding  $\text{CO}_2$  densities were 0.538, 0.709, 0.809  $\text{g mL}^{-1}$ . When the reaction pressure is 165 bar, the reactions achieved high yields with 97.58%, and at higher pressure, the products were isolated with free-flowing powders. Table 3 gives the results of direct overview morphology of the PNIPAM/CMS produced from the reactions with different  $\text{CO}_2$  pressure. When the pressure was increased from 165 to 330 bar, the polymer products mainly distribute dominantly changing from top to bottom, and the higher pressure, the more isolated, the higher particles densities obtained. This suggests that the graft copolymerization of PNIPAM on CMS in  $\text{scCO}_2$  is extremely sensitive to the density of the continuous phase. An interesting behavior was found during the synthesis of copolymers, when the pressure is 165 bar, the polymer filled the whole reactor volume (300 mL). However, the polymer formed a monolith with 40 mm diameter and 10 mm thick cakes in bottom of view autoclave when the pressure was 330 bar. But at 230 bar the polymer is white free-flow powder in bottom of the autoclave.

Table 3  
Effect of reaction pressures on graft copolymerization in  $\text{scCO}_2$

Entry	Pressure (bar)	Conversion (%)	Polymer morphology
10	165	97.58	White soft powder
11	230	82.26	White flow powder
12 <sup>a</sup>	230	16.67	Yellowish particle
13	330	82.26	Monolith

Reaction condition: 0.8 g NIPAM, 0.35 g CMS, 0.05 g AIBN, 0.04 g MBAM, 70 °C, 6 h.

<sup>a</sup> 0 g MBAM.

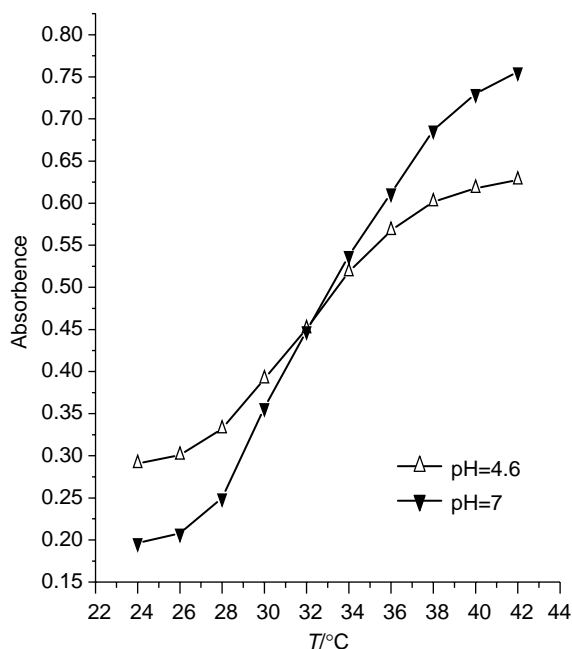


Fig. 7. Light absorbency as a function of temperature ( $\lambda=500$  nm) 0.8 g NIPAM; 0.25 g CMS; 0.025 g crosslinker.

### 3.8. Temperature and pH sensitivities

The volume phase transition temperatures (VPTT) of the core-shell microgels in water were examined by measuring the transmittance of the microgels dispersion as a function of temperature. Fig. 7 shows that the VPTT of the PNIPAM/CMS microgels at pH 4.6 and 7 were almost the same (32 °C). The result strongly suggests that the microgels have a well defined core-shell nanostructure. Hence the properties of core and shell can be altered independently without interfering with each other. The swelling ratio for PNIPAM/CMS in different pH solutions was shown in Fig. 8. The increase of swelling at pH from 2 to 9 was induced by the ionization of carboxymethyl groups ( $\text{CH}_3\text{COO}^-$ ) at pH values above the  $\text{p}K_a$  of CMS, in which the ionic electrostatic repulsion between  $\text{CH}_3\text{COO}^-$  expands the polymer network. At pH above 3.5, significantly

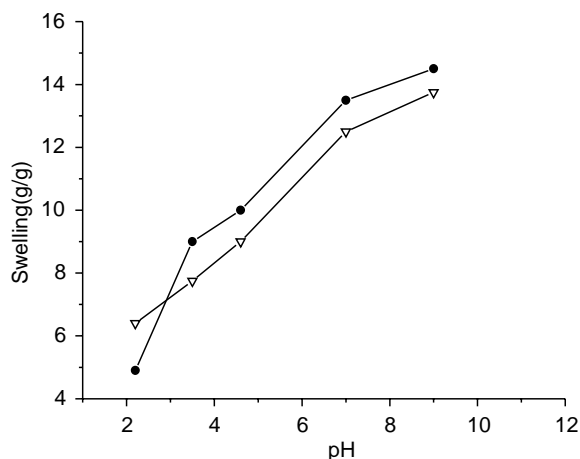


Fig. 8. Effect of pH on swelling ratios condition: 0.8 g NIPAM, 0.04 g MBAM, CMS:  $\nabla$  0.15  $\bullet$  0.25 g.

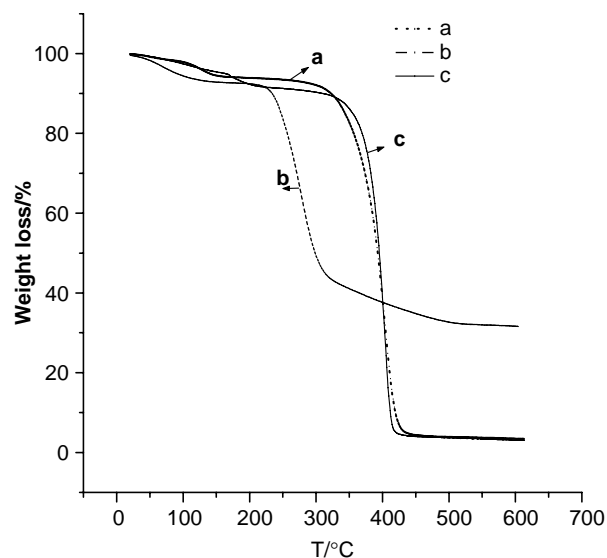


Fig. 9. TGA curves of (a) crosslinked PNIPAM; (b) CMS; (c) copolymer particles (PNIPAM/CMS=4.4/10 w/w; 0.04 g crosslinker; 160 bar).

higher swelling was observed in the microgels with higher CMS contents. These results evidently demonstrate that CMS shells are pH-sensitive, and the thickness of the shell can be easily altered with the change of pH of the dispersing medium.

### 3.9. TGA measurements

Fig. 9 shows the TGA curves of crosslinked PNIPAM, CMS and PNIPAM/CMS. The degradation temperature of CMS was lower than that of crosslinked PNIPAM. Therefore, the degradation temperature of the PNIPAM/CMS copolymer was lower than that of crosslinked PNIPAM. The morphology of poly(NIPAM-CMS) copolymer particles was observed to be a core-shell structure, so the TGA curve of the copolymer fell between those of crosslinked PNIPAM and CMS.

## 4. Conclusion

It was demonstrated that core-shell PNIPAM/CMS micro-particles can be produced in supercritical carbon dioxide through a simple one-step seed polymerization method. CMS, crosslinker effectively worked as surfactant in the stabilization of the PNIPAM/CMS microparticles. It is possible to obtain monodispersed nano-sized spherical particles with narrow size distribution and in short reaction times, by changing the initial concentrations of initiator, crosslinker and CMS dose as well as  $\text{CO}_2$  pressure. The polymers were obtained in high yield as dry, fine and free flowing material directly from the reaction vessel. No contamination of monomer was obtained in the final product by continuously washing the polymer at the end of the reaction with high-pressure  $\text{CO}_2$ . This technically and environmentally satisfying method using  $\text{CO}_2$  as the only solvent is applicable to many combinations of different materials and can lead to the production of a wide variety of new polymer composite microparticle materials.

## References

- [1] DeSimone JM, Guan Z, Elsbernd CS. *Science* 1992;257:945–7.
- [2] Cooper AI. *J Mater Chem* 2000;10:207–34.
- [3] Woods HM, Silva M, Nouvel C, Shakesheff KM, Howdle SM. *J Mater Chem* 2004;14:1663–78.
- [4] Li D, Han BX. *Macromolecules* 2000;33:4555–60.
- [5] Kajimoto O. *Chem Rev* 1999;99:355–90.
- [6] Kendall JL, Canelas DA, Young JL, DeSimone JM. *Chem Rev* 1999;99:543–63.
- [7] Dong ZX, Liu ZM, Han BX, Pei XW, Liu LL, Yang GY. *J Supercrit Fluids* 2004;31:67–74.
- [8] Thurecht KJ, Hill DT, Preston CL, Rintoul L, White JW, Whittaker AK. *Macromolecules* 2004;37:6019–26.
- [9] Alessandro G, Raffaella DG, Giuseppe S, Onofrio S, Giuseppe F. *Macromolecules* 2004;37:4580–9.
- [10] Liu ZM, Dong ZX, Han BX, Wang JQ, He J, Yang GY. *Chem Mater* 2002;14:4619–23.
- [11] Sun DH, Wang B, He J, Zhang R, Liu ZM, Han BX, et al. *Polymer* 2004;45:3805–10.
- [12] Kunita MH, Rinaldi AW, Giroto EM, Radovanovic E, Muniz EC, Rubira AF. *Eur Polym J* 2005;41:2176–82.
- [13] Adamsky FA, Beckman EJ. *Macromolecules* 1994;27:312–4.
- [14] Zhang B, Chen MC, Liu WQ. *Polym Prepr* 2004;45:512–3.
- [15] Ye WJ, DeSimone JM. *Macromolecules* 2005;38:2180–90.
- [16] Galia A, Muratore A, Filardo G. *Ind Eng Chem Res* 2003;42:448–55.
- [17] Yong JL, Spontak RJ, DeSimone JM. *Polym Prepr* 1999;40:829–30.
- [18] Pelton R. *Adv Colloid Interface Sci* 2000;85:1–33.
- [19] Cao ZQ, Liu WG, Gao P, Yao KD, Li HX, Wang GC. *Polymer* 2005;46:5268–77.
- [20] Gao CY, Möhwald H, Shen JC. *Polymer* 2005;46:4088–97.
- [21] Gao HF, Yang WL, Min K, Zha LS, Wang CC, Fu SK. *Polymer* 2005;46:1087–93.
- [22] Hoare T, Pelton R. *Polymer* 2005;46:1139–50.
- [23] Hoare T, Pelton R. *Macromolecules* 2004;37:2544–50.
- [24] Serpe MJ, Yarmey KA, Nolan CM, Lyon LA. *Biomacromolecules* 2005;6:408–13.
- [25] Kim J, Nayak S, Lyon LA. *J Am Chem Soc* 2005;127:9588–92.
- [26] Nolan CM, Reyes CD, Debord JD, Garcia AJ, Lyon LA. *Biomacromolecules* 2005;6:2032–9.
- [27] Hong C, You-Lo H. *J Polym Sci, Part A: Polym Chem* 2004;42:3101–293.
- [28] Yeo SD, Kiran E. *Macromolecules* 2004;37:8239–48.
- [29] Zhang SF, Zhu WQ, Yang JZ. *Fine Chem* 1999;1:53–6.
- [30] Lee CF, Wen CJ, Chiu WY. *J Polym Sci, Part A: Polym Chem* 2003;41:2053–63.
- [31] Lin CL, Chiu WY, Lee CF. *Polymer* 2005;46:10001–92.
- [32] Cooper AI, Hems WP, Holmes AB. *Macromolecules* 1999;32:2156–66.
- [33] Quintero-Ortega IA, Vivaldo-Lima E, Luna-Barcenas G, Alvarado JFI, Louvier-Hernandez JF, Sanchez IC. *Ind Eng Chem Res* 2005;44:2823–44.
- [34] Bunyard CW, Kadla JF, DeSimone JM. *J Am Chem Soc* 2001;123:7199–206.